Middle East Journal of Science

https://dergipark.org.tr/mejs

MEJS

e-ISSN:2618-6136

Research Article

SIMULATION STUDIES OF Cr-doped CuO HETEROJUNCTION SOLAR CELLS

***Serap YIGIT GEZGIN*[1] *Silan BATURAY**[2] *Ilhan CANDAN*[2] *Hamdi Sukur KILIC*[1,3,4]**

[1]Department of Physics, Faculty of Science, University of Selcuk, 42031 Selcuklu, Konya, Turkiye
[2]Department of Physics, Faculty of Science, Dicle University, 21280 Diyarbakir, Turkiye
[3]Direc. of High Technology Research and App. Center, University of Selcuk, 42031 Selcuklu, Konya, Turkiye
[4]Direc. of Laser-Induced Proton Therapy App. and Res. Center, University of Selçuk, 42031 Konya, Turkiye
*Corresponding author: silan@dicle.edu.tr

Abstract: *1% and 3% Cr-doped CuO thin films have been deposited on soda lime glass by the spin coating method, and then their structural, topological, and optical properties have been studied by operating X-ray diffraction, scanning electron microscopy and Ultraviolet-Visible spectroscopy techniques, respectively. XRD patterns of CuO: Cr (1%) and CuO: Cr (3%) thin films demonstrate characteristics of monoclinic CuO structure with a C2/c space group. The morphology of coated film plays an important role in analyzing some optoelectronic properties. 1% Cr-doped CuO thin film absorbs more photons compared to 3% Cr-doped CuO in Vis and UV regions. The band gaps of 1% Cr and 3% Cr-doped CuO thin films are to be 2.18 eV and 2.30 eV, respectively. The Mo/Cr: CuO/SnO_2/n-ZnO/i-ZnO/AZO solar cells have been modeled with the SCAPS-1D simulation program. The photovoltaic parameters of solar cells deteriorated with some increase in the neutral defect density value. As the shallow acceptor defect density value is increased, short-circuit current density (J_{SC}) is decreased, short-circuit current density (V_{OC}), fill factor (FF) and efficiency (η) are increased. The photovoltaic parameters' performance of 1% Cr-doped CuO solar cells was found to be better than that of 3% Cr-doped CuO solar cells. The efficiency of 1% Cr-doped CuO solar cells is increased with the use of a SnO_2 intermediate layer in 2 nm thickness at the heterojunction interface.*

Keywords*: Cr-doped CuO, thin film, solar cells, SCAPS-1D*

Received: April 28, 2023 *Accepted: December 4, 2023*

1. Introduction

The *p*-type copper oxide (CuO) semiconductor has gained much attention in recent years. As a matter of fact, it has presented some attractions in a fundamental way in various areas of science such as chemistry, physics, and material science. Due to being a non-toxic, inexpensive, and easily found raw copper material, CuO is a promising compound [1]. CuO has a monoclinic structure and small optical band gap that varies between 1.56 eV and 2.46 eV [2]. CuO is an exclusive monoxide material for significant surveys as well as many practical applications such as photocatalysis [3, 4], lithium batteries [5], high-Tc superconductor [6-8], gas sensors [9-11], magnetic storage [12], and solar cell applications [13, 14]. Copper oxide has been produced employing numerous methods, including reflux condensation [15, 16], chemical bath deposition [2], sol-gel [17, 18], radio frequency plasma-aided pulsed laser [19], thermal oxidation [20], electrodeposition [21], reactive DC magnetron sputtering [22], evaporation of simple solvent [23] solution casting [24], and spray pyrolysis [25]. The spin coating technique is a deposition procedure that has attracted the research community's significant attention. It has numerous advantages, such as low-cost technique, simplicity, adherent production, effectiveness reproducibility,

stoichiometry, and homogenous deposition of thin films. Furthermore, it does not need a vacuum or sophisticated materials, thus it is very easy to work with. The resistivity of CuO is quite high, and not many studies have been carried out to investigate the nature of substrate influence, which is an important parameter which reduces the resistivity layer. Therefore, layers of CuO/ glass and CuO/SnO_2:F/glass were studied to reveal the impact of substrate nature on CuO thin films' physical characteristics, particularly the investigation of properties related to photovoltaic (PV) applications.

There can be negative factors such as lattice mismatch, interface states, defects and traps, and mismatched band alignment between *p*- and *n*-type semiconductors in a heterojunction solar cell. The SnO_2 intermediate layer can be used to passivate interfacial defects. SnO_2 allows electron transfer while preventing the transition from the absorber layer to the buffer layer. This allows charge collection and increased efficiency in a solar cells [26].

Zinc oxide (ZnO) samples are a binary semiconductor material that have been extensively studied recently due to their excellent electrical, optical, and magnetic properties. They are also highly transparent, have a wide energy band gap value, and are nontoxic. These properties have led to extensive research [27-30]. ZnO thin films typically display *n*-type conduction at Zn rich conditions. It was happened by a deviation from stoichiometry due to 'intrinsic' donors including, oxygen vacancies, H incorporation, and zinc interstitials [29]. On the additional hand, the *p*-type conduction in zinc oxide is usually stated by relatively low hole-mobility and low hole-concentration as well as instability due to the deep acceptor-levels of the dopant element.

Recently, a simulation program employed to determine the solar cell' efficiency with the use of layers that form solar cell has gained significant. One of the most commonly employed programs in this area is SCAPS-1D (one-dimensional simulation software) that calculates a solar cell's PV parameters by parameters including energy band gap, dielectric permittivity, thin film thickness, the layers' electron affinity when constructing the solar cells, the contact material's work function [31, 32]. It was generated at the University of Gent in the Electronics and Information Systems' Department. Depending on Auger electron/hole capture coefficient, interfacial defect density, and operation temperature parameters [33], solar cells' PV parameters can be calculated, and hence, a reliable forecast could be done on the solar cell's performance.

Doping has a large impact on the structural, electrical and optical properties of CuO film. However, a few experimental studies have available on the experimental and photovoltaic calculation for solar cells. Thus, to get more light in understanding of the effect of doping ratio and back contact on physical properties of Cr:CuO film, more experimental and theoretically studies are necessary. We have studied the influences of Cr doping on the structural, topological, optical, and photovoltaic properties of CuO film. In this study, 1% and 3% Cr-doped CuO thin films were fabricated by a system of spin coating. 1% and 3% Cr-doped CuO thin films' structural, topological, and optical properties were examined by X-ray diffraction (XRD), scanning electron microscopy (SEM), and Ultraviolet-Visible spectrophotometry (UV-Vis), respectively. Moreover, by employing SCAPS simulation program, the solar cells consisting of Mo/Cr:CuO/SnO_2/*n*-ZnO/i-ZnO/AZO layers were modelled.

2. Materials and Methods

Analytical-grade precursor copper (II) acetate ($Cu(CH_3COO)_2.H_2O$, 0.1 M) and chromium (III) chloride ($CrCl_3.6H_2O$, 0.01 M) were used in this study. Sufficient $CrCl_3.6H_2O$ was mixed in the $Cu(CH_3COO)_2.H_2O$ to obtain doping concentrations of 1 and 3 at.%, and the liquid dark blue solutions were stirred for 5 h at room temperature. Ethanol and diethanolamine (1:10) were used throughout the experimental procedures as solvents and stabilizers, respectively. Before the coating fabrication process, SLG substrates were firstly boiled in a 5:1:1 deionized water (H_2O), ammonia, and hydrogen peroxide (H_2O_2) mix for a time of around 20 min. at a temperature of ~90 ^{O}C and in a solution of the same ratio

of H_2O, H_2O_2, and hydrogen chloride at the same temperature and time to remove the unnecessary impurities on the SLG substrate [18]. The obtained solutions were deposited on SLG substrates to obtain 1 and 3% Cr-doped CuO films by spin coating method at 1500 rpm for 55 s. After this, the coating thin films were annealed for around 60 min in a furnace at ~500 ^{O}C. The process of spin coating fabrication was optimized for the best fabrication of CuO:Cr thin films, such as the SLG substrate temperature being fixed at 230 ^{O}C. The coated CuO:Cr films were subjected to characterization using advanced techniques. In order to investigate the crystallite parameters, purity, and phase of films, an XRD (Cu-Kα source with wavelength of around 0.154 nm for $\theta - 2\theta$ range in the steps of 0.02^{o}) was used. The surface morphology of the coated Cr:CuO thin films on the soda lime glass (SLG) substrate was studied by scanning electron microscope (a Quanta FEG 250 scanning electron microscope). UV-Vis spectrophotometer (Shimadzu UV-3600, Tokyo, Japan) was used to calculate the absorption data and energy gap in a wavelength range of 300–1100 nm at room temperature. Moreover, 1% and 3% Cr-doped Mo/CuO/*n*-ZnO/i-ZnO/AZO solar cells have been theoretically modelled and the PV parameters of solar cells have been analysed using SCAPD-1D simulation program.

3. Results and Discussion

Figure 1 indicates that XRD patterns of Cr:CuO (1%) and Cr:CuO (3%) thin film demonstrate a characteristic monoclinic CuO structure with a C2/c space group. The diffraction peaks at (-111), (111), (-202), (020), (-311), and (113) are indexed to CuO phase (JCPDS 05-6661). The observed peaks in the high-intensity diffraction spectra suggest that thin films belong to crystallized CuO. Further, the doping ratio changes the XRD pattern of the coated thin film, stating that there is a change of structure in doping in the Cr (1%) and Cr (3%). It can be noticed that the increasing Cr ratio in CuO has made the main peaks more intense.

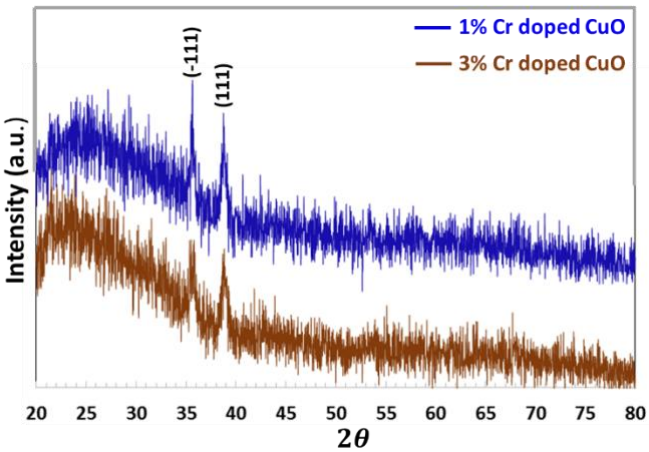

Figure 1. XRD pattern of 1% Cr and 3% Cr-doped CuO thin films.

Our previous study indicates the detailed diffraction information collected from XRD data, including peak orientations (*hkl*), micro- strain (ε), crystallite size (D), dislocation density (δ), and value of inter-planar spacing (d) for (-111) and (111) peaks [18]. The results of the previous study indicate that the crystallite parameters changed due to an increase in Cr ratio. The change in the crystallite parameters by doping metals into CuO has been earlier reported by different research groups [34-36] and matched with our work.

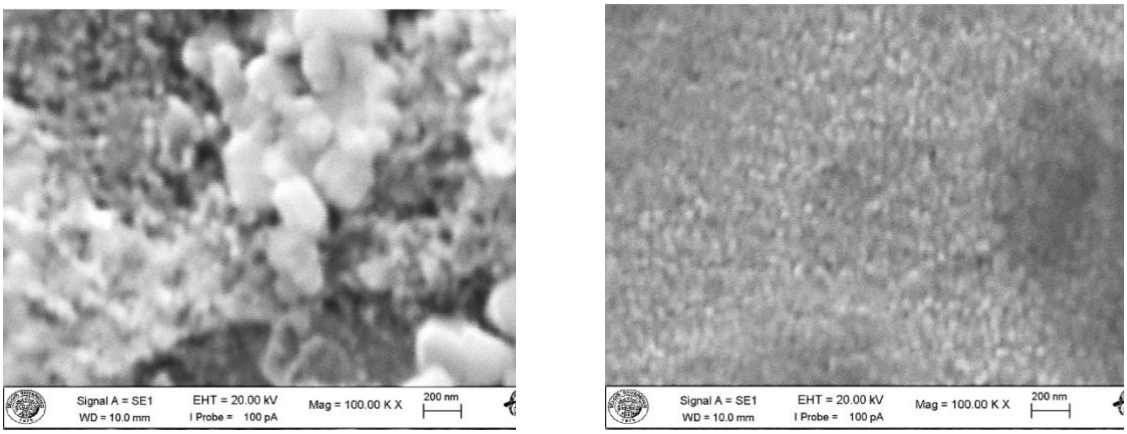

Figure 2. SEM image of **a)** 1% Cr and **b)** 3% Cr-doped CuO thin films.

Figure 2 represents the SEM of Cr:CuO (1%) and Cr:CuO (3%) thin films. The topology of coated film plays an important role in analyzing its optoelectronic properties. An agglomerated morphology can be seen in Figure 2a, whereas a flaky morphology can be realized in Figure 2b. CuO thin films doped with 1% Cr appear slightly different from CuO thin films doped with 3% Cr doping, which is supported by the XRD spectrum. Cr:CuO (1%) and Cr:CuO (3%) thin films exhibit a visible aggregation of particles, showing a little variation in the development of CuO thin films, as shown in the XRD spectrum of thin films. Nanoparticles having the appearance of a flaky ribbon have been widely dispersed over the surface of the substrate, forming a homogenous thin film. These surfaces, which came about as a result of doping CuO thin film, are anticipated to exhibit exceptional optoelectronic capabilities. Dinc et al. indicated that the surface remains homogeneous despite minor clumping caused by Cr-doping. Because of the mild doping, the change in crystallite size is not considerable [37].

3.1. The properties of 1% and 3% Cr-doped CuO thin films

1% Cr-doped CuO thin film absorbs more photons compared to 3% Cr-doped CuO in the visible and UV regions in Figure 3a. The crystallite size of 1% Cr-doped CuO thin film is larger than the crystallite size of 3% Cr-doped CuO thin film, allowing lighter to be absorbed in thin film while limiting its transmission. This shows that 1% Cr-doped CuO thin film is more ideal for use as an absorber layer in PV fields. According to Tauc Plot in the Figures 3b and 3c, the band gaps of 1% Cr and 3% Cr-doped CuO thin films are to be 2.18 eV and 2.30 eV, respectively [18]. Doping with 1% Cr may create shallow defects in the valence band of CuO, which can lead to a decrease in the band gap.

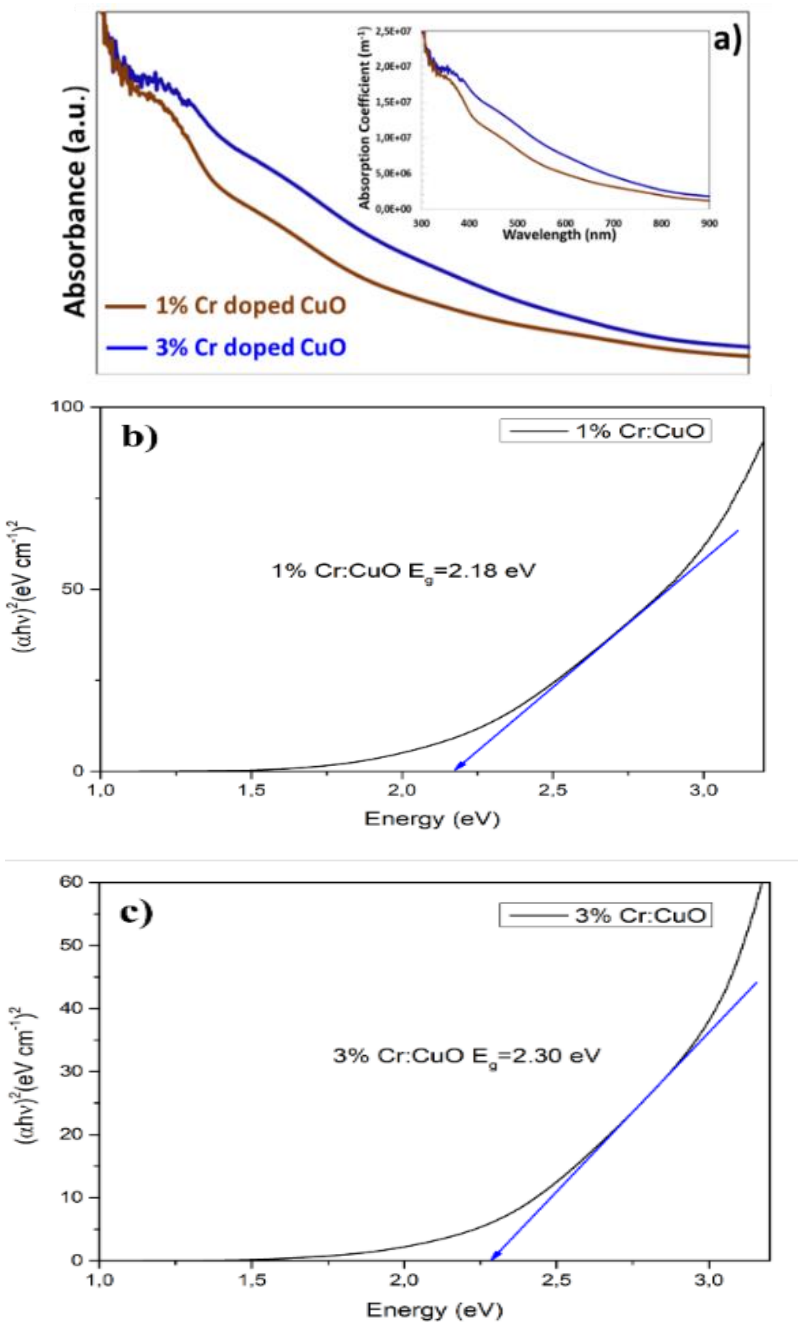

Figure 3. a) The absorbance spectrum **b)** Tauc plot of 1% Cr and **c)** 3% Cr-doped CuO films.

The absorption coefficient (α) of a thin film is expressed by Equation (1) [38]:

$$\alpha = 2.303 * (\frac{A}{W}) \quad (1)$$

A is the absorbance and W is the thin film thickness. 1% Cr-doped CuO thin film indicates a higher absorption coefficient in the Vis and UV regions compared to 3% Cr-doped CuO thin film, as seen in the inset of Figure 3a.

3.2. Modelling of Mo/Cr:CuO/SnO_2/n-ZnO/i-ZnO/AZO thin film solar cells

In this study, SCAPS-1D simulation program [39] was used to model Mo/Cr: CuO/SnO_2/*n*-ZnO/i-ZnO/AZO thin film solar cells as seen Figure 4. In order to model and calculate the electrical parameters of solar cells, the electrical data of all semiconductor layers (given in Table 1) forming the solar cells are input to the program. Experimental data such as band gap, film thickness, absorption coefficient of CuO file (in insert square in Figure 3a) and Cr-doped CuO semiconductors, and values of other layers in literature were used.

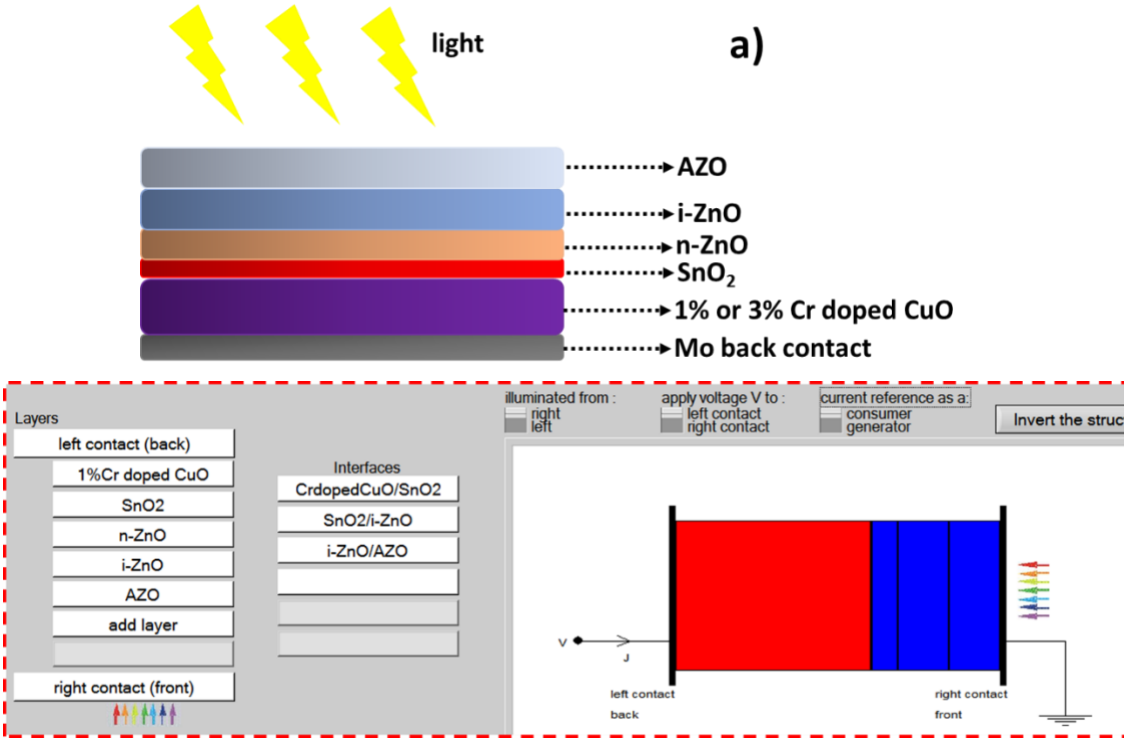

Figure 4. a) The diagram image and **b)** the modelled view of Mo/Cr:CuO/SnO_2/*n*-ZnO/i-ZnO/AZO solar cells.

Table 1. The electrical parameters of semiconductor layers formed Mo/Cr:CuO/SnO_2/*n*-ZnO/i-ZnO/AZO solar cells.

Layers	AZO[40]	i-ZnO [41]	*n*-ZnO	SnO_2	Cr:CuO [42, 43]
Band Gap (eV)	3.3	3.3	3.3	36	2.18/2.30
Electron affinity (eV)	4.6	4.6	4.6	4.5	4.07
Dielectric permittivity (relative)	9	9	9	13.6	11.40/11.43
CB effective density of states (cm^{-3})	$2.20x10^{18}$	$2.20x10^{18}$	$2.20x10^{18}$	$2.20x10^{18}$	$2.20x10^{19}$
VB effective density of states (cm^{-3})	$1.80x10^{19}$	$1.80x10^{19}$	$1.80x10^{19}$	$1.80x10^{19}$	$5.50x10^{20}$
Electron/Hole thermal velocity (cm/s)	$1.00x10^{7}$	$1.00x10^{7}$	$1.00x10^{7}$	$1.00x10^{7}$	$1.00x10^{7}$
Electron/Hole mobility (cm^2/Vs)	100/25	100/25	100/25	100/25	100/20
Shallow donor density (cm^{-3})	$1.00x10^{20}$	$1.00x10^{5}$	0	0	0
Shallow acceptor density (cm^{-3})	0	0	$1.00x10^{18}$	$1.00x10^{16}$	$1.0x10^{16}$
Thickness (nm)	100	100	50	50	380

3.2.1 The effect of the acceptor shallow density (N_a) in Cr:CuO semiconductors on the PV parameters of solar cells

Acceptor defects improve the *p*-type electrical properties of semiconductors. It prevents the recombination of photo-excited charge carriers and increases the number of charge carriers in semiconductors. Thus, a faster and more intense charge transfer takes place in the depletion region. The electrical field increases in the depletion region, and the amount of charge accumulation at the sides increases. Thus, an increase in J_{SC} and V_{OC} value of solar cells occurs [28].

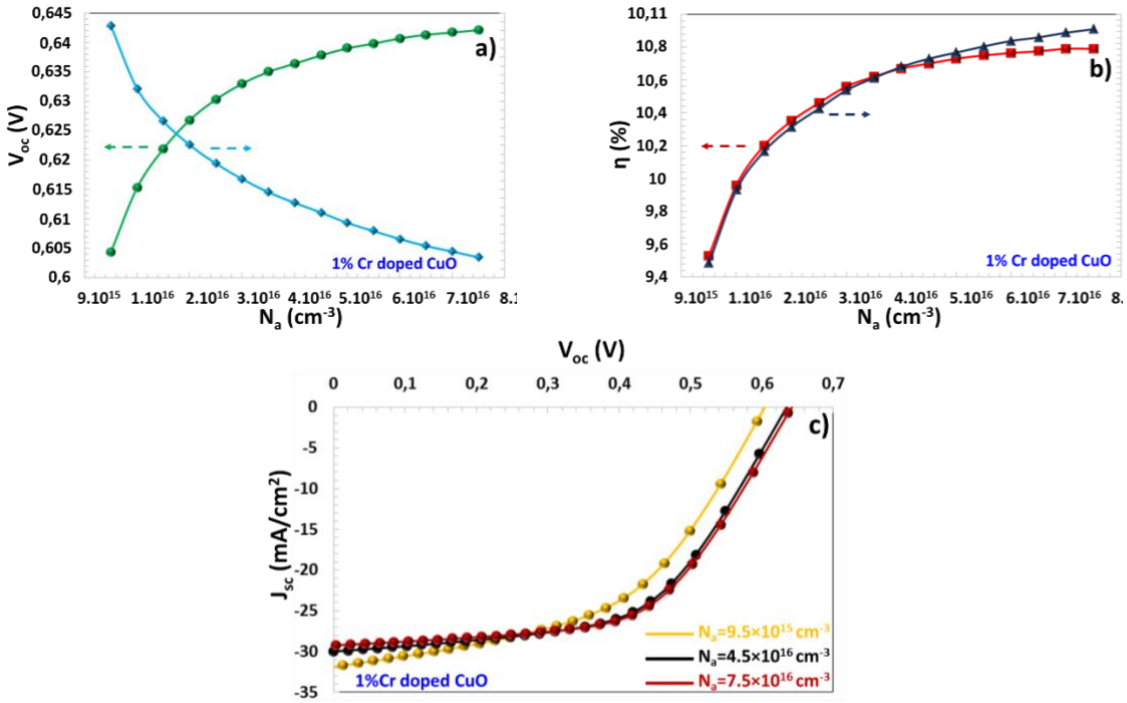

Figure 5. a) ($V_{OC} - J_{SC}$), **b)** (η and FF) vs N_a, and c) $J - V$ for 1% Cr-doped CuO semiconductor.

The N_a dependent ($V_{OC} - J_{SC}$), (η and FF) curves and $J - V$ characteristics of 1% Cr-doped CuO solar cells modelled in this study are given in Figure 5a, 5b and 5c, respectively. As N_a-increased, V_{OC}, η and FF values increased [44], but J_{SC} decreased [45]. Wanda et al indicated that there is a significant potential barrier at the CZTS/Molybdenum interface, as evidenced by the recombination current density at the back-contact, which is estimated to be 3.6 mA/cm^2 [46].This situation can be explained as follows: Some of the photo-excited charge carriers can be trapped by these acceptor defects, and this may cause a decrease in the photocurrent and J_{SC} values. However, since the size of electrical field in the depletion region will cause charge separation, it will increase the charge accumulation at the boundaries of the depletion region and lead to the other PV values to increase [38, 47]. As N_a increases from 9.5×10^{15} cm^{-3} to 7.5×10^{16} cm^{-3}, J_{SC}, V_{OC}, FF and η parameters of 1% Cr:CuO solar cells changed from 31.85 mA/cm^2 to 29.23 mA/cm^2, from 0.604 mV to 0.642 mV, from 49.48% to 57.49%, and from 9.53% to 10.79%, respectively. Adewoyin et al. reported that with an efficiency of 9.39%, the composition ratio of $Cu_2ZnSn_{0.8}Ge_{0.2}S_4$ produced the best $J-V$ characteristics of the top cell, which is lower than our calculated value [40].

The solar cell has shown the highest power conversion efficiency for N_a =7.5×10^{16} cm^{-3}. According to the curves in Figure 6, when the value of N_a increased from 9.5×10^{15} cm^{-3} to 5×10^{16} cm^{-3}, V_{OC}, J_{SC}, FF and η values of 3% Cr:CuO solar cells have been changed from 26.01 mA/cm^2 to 23.92

mA/cm^2, from 0.552 mV to 0.571 mV, from 51.55% to 57.7% and from 7.41% to 7.9%, respectively. Thus, 3% Cr:CuO solar cells exhibits the lower efficiency compared to 1% Cr-doped CuO solar cells. 3% Cr:CuO thin film contains more defects than the other. Also, since 3% Cr-doped CuO thin film absorbs fewer photons, fewer photo-excited charge carriers are formed in the film, resulting in lower efficiency of solar cells.

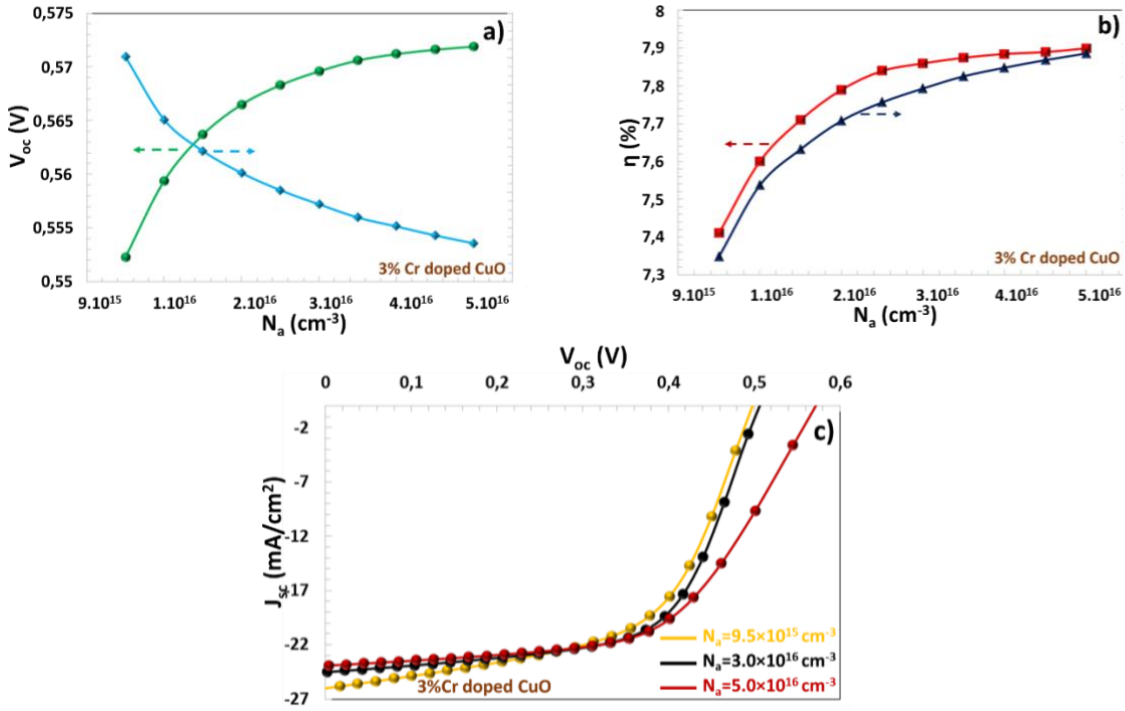

Figure 6. a) ($V_{OC} - J_{SC}$), **b)** (η and FF) vs N_a, and **c)** $J - V$ for 3 % Cr: CuO semiconductor.

3.2.2 The effect of the neutral interface defect density (N_t) in 1% Cr-doped CuO semiconductor on the PV parameters of the solar cells

The defects located between the absorber layer and the buffer layer in the solar cell significantly affect the efficiency of the solar cell. Factors such as lattice mismatch of semiconductors in heterojunction, mismatched band alignment, bond hanging, and doping in the depilation region can cause interface defects [48]. These defects can act as recombination points for electron and hole pairs. The charge transitions are limited by being positioned close to the band edges. Therefore, with increasing defect density, charge accumulation in the depletion region of solar cells decreases, and this causes a decrease in PV parameters [33, 38, 39].

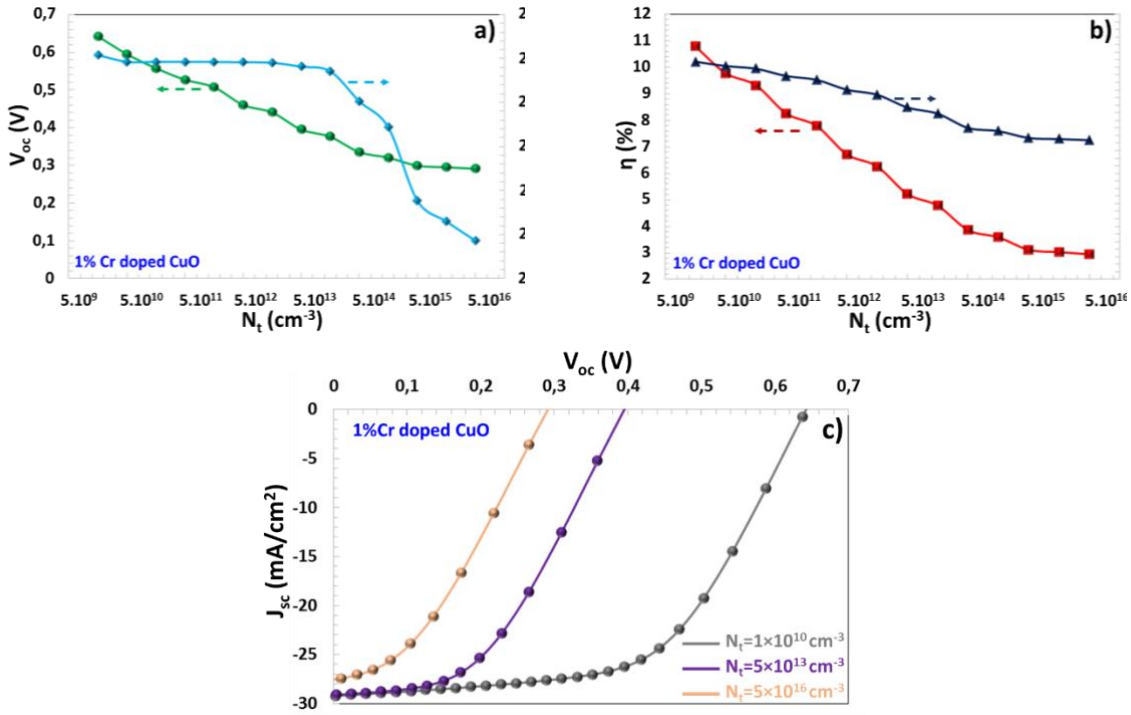

Figure 7. a) ($V_{OC} - J_{SC}$), **b)** (η and FF) vs N_t, and **c)** $J - V$ for 1% Cr:CuO semiconductor.

In this study, since %1 Cr-doped CuO solar cell exhibits higher efficiency, efficiency improvement studies have been carried out on this solar cell. The N_t (neutral defect density) dependent ($V_{OC} - J_{SC}$), (η and FF) curves and $J - V$ characteristics of 1% Cr-doped CuO solar cells have been modelled in the study and are given in Figure 7a, 7b and 7c, respectively. While N_t increases, all electrical parameters of the solar cells decrease. So, N_t rises from 1.0×10^{10} cm^{-3} to 5×10^{16} cm^{-3}, ($V_{OC} - J_{SC}$), (η and FF) values of 1% Cr-doped CuO solar cells have been decreased from 29.23 mA/cm^2 to 27.54 mA/cm^2, from 0.642 mV to 0.291 mV, from 57.49% to 36.75% and from 10.79% to 2.95%, respectively. 1% Cr-doped CuO solar cells has shown the highest power conversion efficiency for N_t =1.0×10^{10} cm^{-3}.

3.2.3 The effect of the SnO_2 layer on the PV performance of 1% Cr:CuO solar cells

According to the band diagram of 1%Cr-doped CuO solar cells in Figure 8a, a cliff-like band [42] was formed between the 1% Cr-doped CuO and the *n*-ZnO heterojunction. A cliff-like conduction band offset leads to trap state-assisted recombination. This causes the charge carriers to decrease and J_{SC} value to deteriorate. In this study, to overcome this problem, a SnO_2 ultrathin intermediate layer in the 3.6 eV band gap [42] that was placed between as shown in the band diagram in Figure 8b. The SnO_2 layer partially forms a spike like conduction band offset, optimizing conduction band alignment. It prevents recombination caused by trap states at the interface [26, 49]. Therefore, SnO_2 blocks the hole charges away from the ZnO buffer layer, which acts as an electron selector for the 1% Cr:CuO active layer as seen in Figure 8c, in order to passivate the interface states.

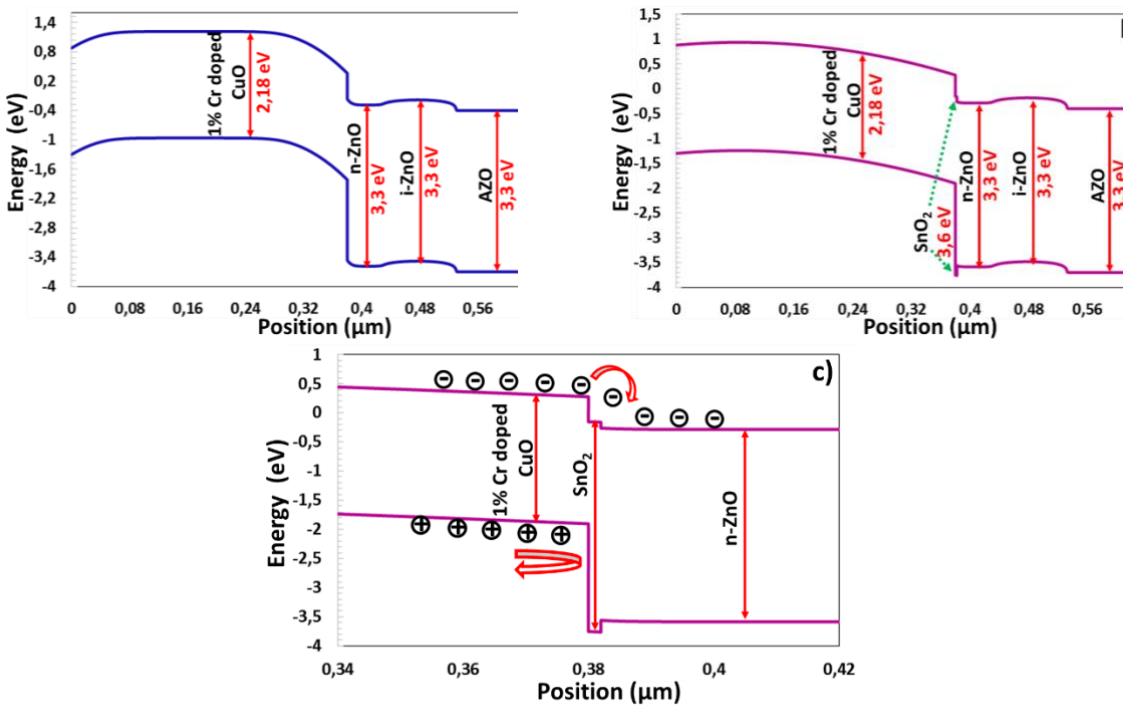

Figure 8. a) The band diagrams of 1% Cr: CuO/*n*-ZnO, **b)** 1% Cr: CuO/SnO_2/*n*-ZnO solar cells and **c)** the charge transfer in 1% Cr:CuO solar cells with SnO_2 intermediate layer.

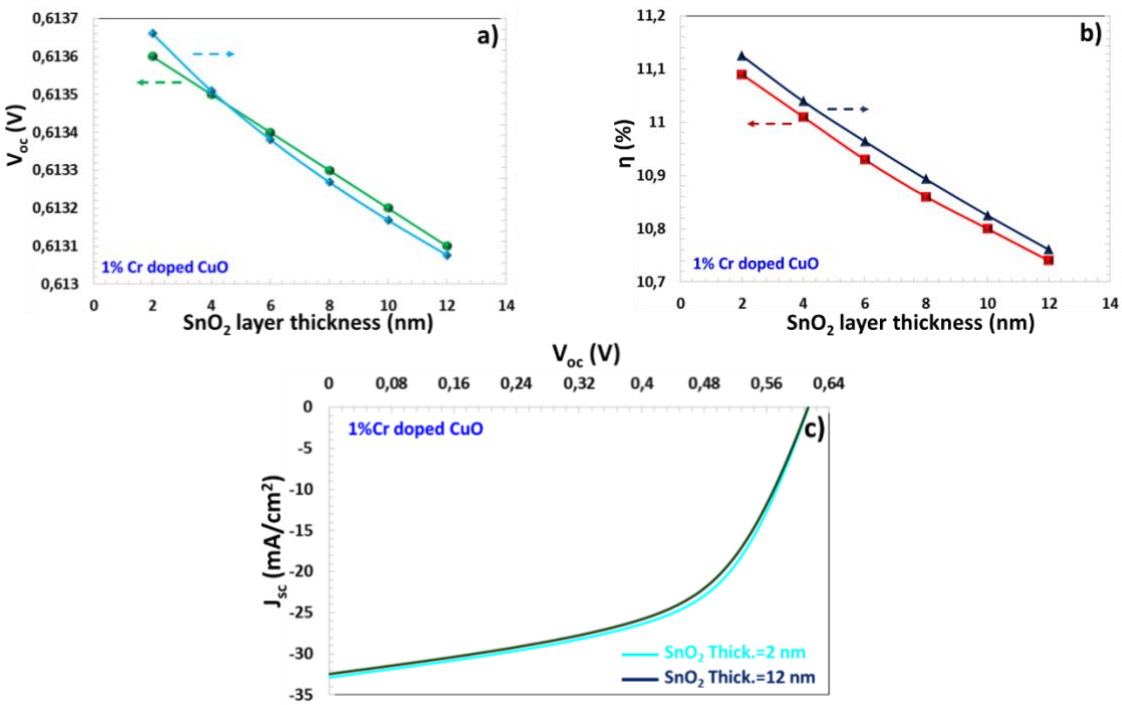

Figure 9. a) ($V_{OC} - J_{SC}$), **b)** (η and FF) vs SnO_2 layer thickness graphs and **c)** $J - V$ characteristics dependent SnO_2 layer thickness for 1% Cr-doped CuO semiconductor.

Figure 9 show that ($V_{OC} - J_{SC}$), (η and FF) vs SnO_2 layer thickness graphs and $J - V$ characteristics-dependent SnO_2 layer thickness (for 2 nm and 12 nm) for 1% Cr:CuO semiconductor. For the solar cells with SnO_2 layer thickness of 2 nm, (J_{SC} =32.9 mA/cm^2, V_{OC} =0.615 mV, FF =54.99% and $\eta = 11.09\%$ while J_{SC} =29.23mA/cm^2, V_{OC} =0.642 mV, FF =57.49% and

η =10.79% to solar cells without SnO_2 layer. Sun et al. indicate that CZTS solar cells with SnO_2 intermediate layers have an improved overall efficiency of 6.82% to 8.47% due to their higher V_{OC} of 657 mV and FF of 62.8% when compared to their counterpart cells without the SnO_2 intermediate layer, which have V_{OC} of 638 mV and FF of 52.4% [30]. As stated above, SnO_2 layer provided the ideal charge transition in the band structure. Thus, the photo-excited charge carriers in the depletion region contribute to charge aggregation at the edges and do not adversely affect the shunt resistance, resulting in higher J_{SC} and efficiency values. However, although SnO_2 layer thickness of 2 nm is low, it can cause a large electrical field in the depletion region and trap states for charge carriers in the band gap. This causes V_{OC} and FF values to be slightly lower. However, the high J_{SC} value resulted in higher efficiency compared to η value of solar cells without SnO_2 layer. As SnO_2 film thickness increases from 2 nm to 12 nm, J_{SC}, V_{OC}, FF and η values of 1% Cr-doped CuO solar cells with SnO_2 layer decreases from 32.87 mA/cm^2 to 32.45 mA/cm^2, from 0.613,6 mV to 0.613,1 mV, from 54.99% to 53.97% and from 11.09% to 10.74%, respectively. The higher thickness of SnO_2 layer reduces the electrical field in the depletion region and may limit charge separation. Thus, in interfacial trap states, charge carriers may undergo recombination resulting in degradation of PV performance.

4. Conclusions

In this study, 1% and 3% Cr-doped CuO thin film has been produced by spin coating system. XRD spectra indicates that all of thin films coated had a polycrystalline nature, with preferential (-111) and (111) orientations. Cr doping ratio changes XRD pattern of thin film coated and increments in Cr ratio in CuO have made the main peaks more intense. SEM images reveals that the agglomerated morphology can be seen in CuO:Cr (1%), whereas flaky morphology can be seen in CuO:Cr (3%). 1% Cr-doped CuO thin film absorbs more photons compared to 3% Cr-doped CuO in Vis and UV regions. The band gaps of 1% Cr and 3% Cr-doped CuO thin films have been determined to be 2.18 eV and 2.30 eV, respectively. Using the SCAPS simulation program, the solar cells consisting of Mo/1% and 3% Cr-doped Mo/Cr:CuO/SnO_2/*n*-ZnO/i-ZnO/AZO layers have been modelled. With some increases in N_t neutral defect density, all PV parameters of these solar cells deteriorated. However, 1% Cr-doped CuO solar cells performed better than 3% Cr:CuO solar cells. With the increase of N_a acceptor defect density, while J_{SC} value decreased, V_{OC}, FF and η values of 1% Cr-doped CuO solar cells increased. At the interface, SnO_2 intermediate thin layer with thickness between 2 nm and 12 nm that was put on the interface to passivate the defect, trap structures, and to provide ideal charge transfer (hole and electron). The solar cells with SnO_2 intermediate layer at 2 nm thickness showed higher J_{SC} , FF and η values compared to solar cells without any intermediate layer.

Ethical statement:

The authors declare that this study does not require ethics committee approval or any special permission.

Acknowledgements:

Authors would kindly like to thank to

- Selcuk University, Scientific Research Projects (BAP) Coordination Office for the support with the number 15201070 and 19401140 projects,
- Selçuk University, High Technology Research and Application Center (İL-TEK) and
- SULTAN Center for infrastructures
- Dicle University Scientific Research Project (BAP) Coordination office
- Dr. Marc Burgelman's group, University of Gent, Belgium for providing permission for us to use SCAPS-1D simulation program.

Conflict of interest:

The authors declare no conflicts of interest.

Authors' Contributions:

S. Y. G: Conceptualization, Formal analysis, Writing first draft preparation (30%)
S. B: Conceptualization, Methodology, Resources (%25).
I.C: Formal analysis, draft preparation (%20)
H. S. K: Formal analysis, draft preparation, project coordinator (%25)
All authors read and approved the final manuscript.

References

[1] Sultana, J., Das, A., Saha, N. R., Karmakar, A., and Chattopadhyay, S., "Characterization of nano-powder grown ultra-thin film p-CuO/n-Si hetero-junctions by employing vapour-liquid-solid method for photovoltaic applications," *Thin Solid Films*, 612, 331-336, 2016.

[2] Sultana, J., Paul, S., Karmakar, A., Yi, R., Dalapati, G. K., and Chattopadhyay, S., "Chemical bath deposited (CBD) CuO thin films on n-silicon substrate for electronic and optical applications: Impact of growth time," *Applied surface science*, 418, 380-387, 2017.

[3] Salari, H., and Sadeghinia, M., "MOF-templated synthesis of nano Ag2O/ZnO/CuO heterostructure for photocatalysis," *Journal of Photochemistry and Photobiology A: Chemistry*, 376, 279-287, 2019.

[4] Sharma, D., Prajapati, A. K., Choudhary, R., Kaushal, R. K., Pal, D., and Sawarkar, A. N., "Preparation and characterization of CuO catalyst for the thermolysis treatment of distillery wastewater," *Environmental technology*, 39(20), 2604-2612, 2018.

[5] Zhang, Y., *et al.*, "CuO@ Ag core-shell material preparation and as high-stability anodes for lithium-ion batteries," *Powder Technology*, 355, 386-392, 2019.

[6] Eibl, O., "Application of a new method for absorption correction in high-accuracy, quantitative EDX microanalysis in the TEM: analysis of oxygen in CuO-based high-Tc superconductors," *Ultramicroscopy*, 50(2), 189-201, 1993.

[7] Lokhande, P. E., and Chavan, U. S., "Surfactant-assisted cabbage rose-like CuO deposition on Cu foam by for supercapacitor applications," *Inorganic and Nano-Metal Chemistry*, 48(9), 434-440, 2018.

[8] Ates, M., Garip, A., Yörük, O., Bayrak, Y., Kuzgun, O., and Yildirim, M., "rGO/CuO/PEDOT nanocomposite formation, its characterisation and electrochemical performances for supercapacitors," *Plastics, Rubber and Composites*, 48(4), 168-184, 2019.

[9] Park, K.-R., Cho, H.-B., Lee, J., Song, Y., Kim, W.-B., and Choa, Y.-H., "Design of highly porous SnO2-CuO nanotubes for enhancing H2S gas sensor performance," *Sensors and Actuators B: Chemical*, 302, 127179, 2020.

[10] Shaban, M., Abdelkarem, K., and El Sayed, A. M., "Structural, optical and gas sensing properties of Cu2O/CuO mixed phase: effect of the number of coated layers and (Cr+ S) co-Doping," *Phase Transitions*, 92(4), 347-359, 2019.

[11] Budhiraja, N., Kumar, V., Tomar, M., Gupta, V., and Singh, S., "Facile synthesis of porous CuO nanosheets as high-performance NO2 gas sensor," *Integrated Ferroelectrics*, 193(1), pp. 59-65, 2018.

[12] Sheikholeslami, M., "Solidification of NEPCM under the effect of magnetic field in a porous thermal energy storage enclosure using CuO nanoparticles," *Journal of Molecular Liquids,* 263, 303-315, 2018.

[13] Tan, R., *et al.*, "Enhanced open-circuit photovoltage and charge collection realized in pearl-like NiO/CuO composite nanowires based p-type dye sensitized solar cellss," *Materials Research Bulletin,* 116, 131-136, 2019.

[14] Ayed, R. B., Ajili, M., Thamri, A., Kamoun, N. T., and Abdelghani, A., "Substrate temperature effect on the crystal growth and optoelectronic properties of sprayed α-Fe2O3 thin films: application to gas sensor and novel photovoltaic solar cells structure," *Materials Technology,* 33(12), 769-783, 2018.

[15] Mageshwari, K., Sathyamoorthy, R., and Park, J., "Photocatalytic activity of hierarchical CuO microspheres synthesized by facile reflux condensation method," *Powder Technology,* 278, 150-156, 2015.

[16] Elango, M., Deepa, M., Subramanian, R., and Mohamed Musthafa, A., "Synthesis, characterization, and antibacterial activity of polyindole/Ag–Cuo nanocomposites by reflux condensation method," *Polymer-Plastics Technology and Engineering,* 57(14), 1440-1451, 2018.

[17] Joseph, A., *et al.*, "An experimental investigation on pool boiling heat transfer enhancement using sol-gel derived nano-CuO porous coating," *Experimental Thermal and Fluid Science,* 103, 37-50, 2019.

[18] Baturay, S., Candan, I., and Ozaydın, C., "Structural, optical, and electrical characterizations of Cr-doped CuO thin films," *Journal of Materials Science: Materials in Electronics,* 33(9), 7275-7287, 2022.

[19] Liu, X., Xu, W., Xu, M., Hao, X., and Feng, X., "Epitaxial CuO thin films prepared on MgAl2O4 (110) by RF-plasma assisted pulsed laser deposition," *Vacuum,* 169, 108932, 2019.

[20] Tang, C., Sun, F., Chen, Z., Chen, D., and Liu, Z., "Improved thermal oxidation growth of non-flaking CuO nanorod arrays on Si substrate from Cu film and their nanoscale electrical properties for electronic devices," *Ceramics International,* 45(12), 14562-14567, 2019.

[21] Mahmood, A., Tezcan, F., and Kardaş, G., "Photoelectrochemical characteristics of CuO films with different electrodeposition time," *International journal of hydrogen energy,* 42(36), 23268-23275, 2017.

[22] Sahu, A. K., Das, A., Ghosh, A., and Raj, S., "Understanding blue shift of the longitudinal surface plasmon resonance during growth of gold nanorods," *Nano Express,* 2(1), 010009, 2021.

[23] Aslam, M., Raza, Z. A., and Siddique, A., "Fabrication and chemo-physical characterization of CuO/chitosan nanocomposite-mediated tricomponent PVA films," *Polymer Bulletin,* 78, 1955-1965, 2021.

[24] Aslam, M., Kalyar, M. A., and Raza, Z. A., "Fabrication of nano-CuO-loaded PVA composite films with enhanced optomechanical properties," *Polymer Bulletin,* 78, 1551-1571, 2021.

[25] Shinde, S., *et al.*, "Effect of deposition parameters on spray pyrolysis synthesized CuO nanoparticle thin films for higher supercapacitor performance," *Journal of Electroanalytical Chemistry,* 850, 113433, 2019.

[26] Sun, H., *et al.*, "Efficiency enhancement of kesterite Cu_2ZnSnS_4 solar cellss via solution-processed ultrathin tin oxide intermediate layer at absorber/buffer interface," *ACS Applied Energy Materials*, 1(1), 154-160, 2017.

[27] Pearton, S., Norton, D., Ip, K., Heo, Y. and Steiner, T., "Recent advances in processing of ZnO", *Journal of Vacuum Science&Technology B: Microelectronics and Nanometer Structures Processing, Measurement, and Phenomena*, 22, 932–48, 2004

[28] Look, D.C., "Recent advances in ZnO materials and devices", *Materials Science and Engineering: B* 80, 383–7, 2001

[29] Van de Walle, C.G ., "Hydrogen as a cause of doping in zinc oxide", *Physical Review Letters*, 85, 1012, 2000

[30] Look, D.C., Hemsky, J.W, and Sizelove, J., "Residual native shallow donor in ZnO", *Physical Review Letters*, 82, 2552, 1999

[31] Piñón Reyes, A. C., *et al.*, "Study of a lead-free perovskite solar cell using CZTS as HTL to achieve a 20% PCE by SCAPS-1D simulation," *Micromachines*, 12(12), 1508, 2021.

[32] AlZoubi, T., Moghrabi, A., Moustafa, M., and Yasin, S., "Efficiency boost of CZTS solar cellss based on double-absorber architecture: Device modeling and analysis," *Solar Energy*, 225, 44-52, 2021.

[33] Houimi, A., Gezgin, S. Y., Mercimek, B., and Kılıç, H. Ş., "Numerical analysis of CZTS/n-Si solar cellss using SCAPS-1D. A comparative study between experimental and calculated outputs," *Optical Materials*, 121, 111544, 2021.

[34] Gnanasekar, T., *et al.*, "Enhanced opto-electronic properties of X-doped (X= Al, Ga, and In) CuO thin films for photodetector applications," *Journal of Materials Science: Materials in Electronics*, 33(23), 18786-18797, 2022.

[35] Naveena, D., Logu, T., Dhanabal, R., Sethuraman, K., and Bose, A. C., "Comparative study of effective photoabsorber CuO thin films prepared via different precursors using chemical spray pyrolysis for solar cells application," *Journal of Materials Science: Materials in Electronics*, 30, 561-572, 2019.

[36] Devi, L. V., Selvalakshmi, T., Sellaiyan, S., Uedono, A., Sivaji, K., and Sankar, S., "Effect of La doping on the lattice defects and photoluminescence properties of CuO," *Journal of Alloys and Compounds*, 709, 496-504, 2017.

[37] Dinc, S., Şahin, B., and Kaya, T., "Improved sensing response of nanostructured CuO thin films towards sweat rate monitoring: effect of Cr doping". *Materials Science in Semiconductor Processing*, 105, 104698, 2020

[38] Gezgin, S. Y., "Modelling and investigation of the electrical properties of CIGS/n-Si heterojunction solar cellss," *Optical Materials*, 131, 112738, 2022.

[39] Yiğit Gezgin, S., and Kiliç, H. Ş., "The effect of Ag plasmonic nanoparticles on the efficiency of CZTS solar cells: an experimental investigation and numerical modelling," *Indian Journal of Physics*, **97**(3), 779-796, 2023.

[40] Adewoyin, A. D., Olopade, M. A., Oyebola, O. O., and Chendo, M. A., "Development of CZTGS/CZTS tandem thin film solar cells using SCAPS-1D," *Optik*, 176, 132-142, 2019.

[41] AlZoubi, T., and Moustafa, M., "Numerical optimization of absorber and CdS buffer layers in CIGS solar cellss using SCAPS," *Int. J. Smart Grid Clean Energy,* 8, 291-298, 2019.

[42] Lam, N. D., "Modelling and numerical analysis of ZnO/CuO/Cu_2O heterojunction solar cells using SCAPS," *Engineering Research Express,* 2(2), p. 025033, 2020.

[43] Gezgin, S. Y., Candan, I., Baturay, S., Kilic, H. S., "Structural, Morphological, Optical Properties and Modelling of Ag Doped CuO/ZnO/AZO Solar Cells," *Journal of Coating Science and Technology,* 9, 26-37, 2022/11/21.

[44] Djinkwi Wanda, M., Ouédraogo, S., Tchoffo, F., Zougmoré, F., and Ndjaka, J., "Numerical investigations and analysis of Cu_2ZnSnS_4 based solar cellss by SCAPS-1D," *International Journal of Photoenergy,* 2016, 2016.

[45] Gupta, G. K., and Dixit, A., "Simulation studies of CZT (S, Se) single and tandem junction solar cellss towards possibilities for higher efficiencies up to 22%," *arXiv preprint arXiv:1801.08498,* 2018.

[46] Gezgin, S. Y., Candan, İ., Baturay, Ş., and Kiliç, H. Ş., "Modelling Of The Solar Cell Based On Cu_2SnS_3 Thin Film Produced By Spray Pyrolysis," *Middle East Journal of Science,* 8(1), 64-76, 2022.

[47] Kaur, K., Kumar, N., and Kumar, M., "Strategic review of interface carrier recombination in earth abundant Cu–Zn–Sn–S–Se solar cells: current challenges and future prospects," *Journal of Materials Chemistry A,* 5(7), 3069-3090, 2017.

[48] Mounkachi, O., *et al.*, "Band-gap engineering of SnO_2," *Solar Energy Materials and Solar Cellss,* 148, 34-38, 2016.

[49] Guirdjebaye, N., Ngoupo, A. T., Ouédraogo, S., Tcheum, G. M., and Ndjaka, J., "Numerical analysis of CdS-CIGS interface configuration on the performances of Cu(In,Ga)Se_2 solar cells," *Chinese Journal of Physics,* 67, 230-237, 2020.